AGU PUBLICATIONS

Geophysical Research Letters

RESEARCH LETTER

10.1002/2014GL059244

Key Points:
- Bio-Argo floats can track small particles in the mesopelagic region
- Export fluxes from small particles were significant
- Small particles contributed to long-term carbon sequestration

Supporting Information:
- Text S1
- Text S2

Correspondence to:
G. Dall'Olmo,
gdal@pml.ac.uk

Citation:
Dall'Olmo, G., and K. A. Mork (2014), Carbon export by small particles in the Norwegian Sea, *Geophys. Res. Lett.*, *41*, doi:10.1002/2014GL059244.

Received 13 FEB 2014
Accepted 7 APR 2014
Accepted article online 8 APR 2014

Carbon export by small particles in the Norwegian Sea

Giorgio Dall'Olmo[1,2] and Kjell Arne Mork[3,4]

[1]Plymouth Marine Laboratory, Plymouth, UK, [2]National Centre for Earth Observation, Plymouth, UK, [3]Institute for Marine Research, Bergen, Norway, [4]Centre for Climate Dynamics, Bergen, Norway,

Abstract Despite its fundamental role in controlling the Earth's climate, present estimates of global organic carbon export to the deep sea are affected by relatively large uncertainties. These uncertainties are due to lack of observations as well as disagreement among methods and assumptions used to estimate carbon export. Complementary observations are thus needed to reduce these uncertainties. Here we show that optical backscattering measured by Bio-Argo floats can detect a seasonal carbon export flux in the Norwegian Sea. This export was most likely due to small particles (i.e., 0.2–20 μm), was comparable to published export values, and contributed to long-term carbon sequestration. Our findings highlight the importance of small particles and of physical mixing in the biological carbon pump and support the use of autonomous platforms as tools to improve our mechanistic understanding of the ocean carbon cycle.

1. Introduction

The export of particles from the surface to the deep ocean affects nutrient distributions, sustains mesopelagic and bathypelagic organisms, and, ultimately, contributes to controlling the Earth's climate [*Trull et al.*, 2008]. Despite the importance of this process, however, modern estimates of global carbon export vary between 5 and 12 Pg C yr^{-1} [*Laws et al.*, 2000; *Henson et al.*, 2011]. This large range of variation reflects an ignorance arising from lack of observations and from substantial disagreement among the different methods and assumptions used to estimate the magnitude of export. To predict how oceanic carbon uptake will evolve in the future and to interpret past records of CO_2, we need to understand the factors that control the uncertainty of our current estimates of global carbon export.

In situ optical scattering instruments mounted on autonomous platforms such as Bio-Argo floats can provide observations that are complementary to existing methods for estimating carbon export. These autonomous platforms are advantageous because they allow measurements over sustained periods of time in remote and/or hazardous ocean regions [*Bishop and Wood*, 2009].

Particulate optical backscattering (b_{bp}) is sensitive to marine particles in the approximate size range 0.2–20 μm [*Stramski et al.*, 2004] (see also supporting information) and is correlated to the concentration of particulate organic carbon (POC) [e.g., *Cetinić et al.*, 2012]. When b_{bp} is measured from autonomous platforms, one can estimate the vertically-resolved and time-varying fields needed to study the dynamics of POC in the water column [*Briggs et al.*, 2011].

Here we focus on b_{bp} profiles measured by Bio-Argo floats in the Norwegian Sea. We show that these signals can track the integrated stocks of small marine particles in the euphotic and mesopelagic zones. We further estimate vertically resolved POC export fluxes and transfer efficiencies.

2. Methods

The Lofoten Basin is a deep (~3000 m) region of the open Norwegian Sea (Figure 1). In this basin the bathymetry-driven middepth flow typically forces Argo floats to remain in the basin of deployment, even after multiple years of operation [*Voet et al.*, 2010]. Thus, this deep basin is ideal to conduct pilot studies using biogeochemical floats.

Two Teledyne Webb Autonomous Profiling Explorer floats equipped with conductivity-temperature-depth and WETLabs sensors for measuring chlorophyll fluorescence (chl) and optical backscattering at 700 nm collected data from 2010 to 2012 in the Lofoten Basin (Figure 1). The floats were programmed to surface every 10 days during the winter and every 5 days in the summer (see also supporting information).

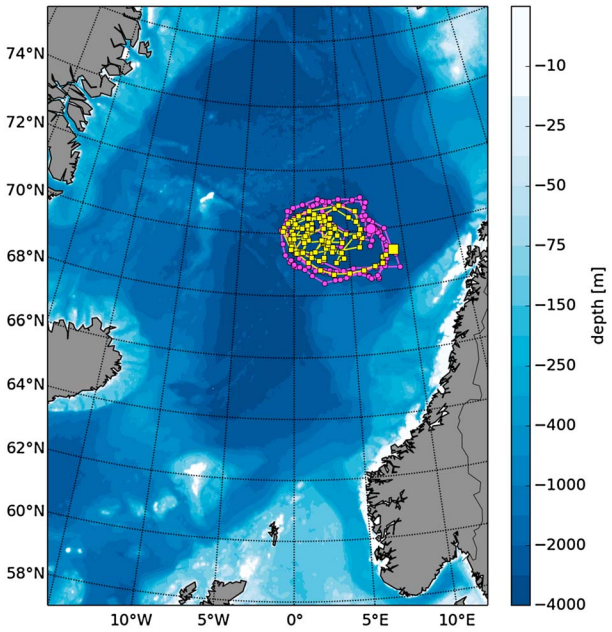

Figure 1. Bathymetric map of the Nordic Seas with the locations of profiles from Argo floats 6900798 and 6900799 (yellow and magenta symbols and lines, respectively) in the Lofoten Basin. Larger symbols indicate the locations of the last measurements. Profile times ranged from every 5 days in the spring-summer to every 10 days during late autumn and winter.

Manufacturer-supplied offsets and scaling factors were applied to raw fluorescence and backscattering data. Particulate backscattering (b_{bp}) was then computed following established protocols [e.g., *Dall'Olmo et al.*, 2012]. To account for biases in the dark offsets, the minimum b_{bp} value measured by each float ($\sim 5 \times 10^{-4}$ m^{-1}) was removed from the corresponding time series (note that this subtraction may cause an underestimation of POC, see below). High-frequency spikes were further removed from the b_{bp} data using a median filter. Finally, b_{bp} was used to estimate the concentration of particulate organic carbon (POC) using empirical conversion factors published for the North Atlantic. Different values were used within and below the mixed layer: 37, 530 and 31, 620 mg POC m^{-2}, respectively [*Cetinić et al.*, 2012].

Estimates of mixed layer depth (z_m) were computed as the depth at which potential density decreased by 0.10 kg m^{-3} from the surface layer [e.g., *Bagoien et al.*, 2012]. The depth of the bottom of the euphotic zone (z_{eu}) was computed based on an empirical relationship that was established between float-based surface chl and Moderate Resolution Imaging Spectroradiometer (MODIS) AQUA remote sensing estimates of z_{eu} (supporting information). Finally, the thickness of the layer where particles can potentially be produced by photosynthesis (z_p) was computed as the maximum of z_{eu} and z_m.

Particulate organic carbon values were integrated over various depths including the sampled water column ($0 - 1000$ m, $iPOC_0^{1000}$), the "productive layer" ($0 - z_p$ m, $iPOC_0^{z_p}$), the "mesopelagic layer" ($z_p - 1000$ m, $iPOC_{z_p}^{1000}$), as well as over progressively deeper parts of the mesopelagic layer ($iPOC_{z_p+z_i}^{1000}$, with z_i = [50, 100, 200, 300, 400] m).

Assuming spatial homogeneity and a negligible POC flux at 1000 m, the time rate of change of iPOC integrated from z_i meters below z_p to 1000 m, $E_{z_i} = \partial iPOC_{z_p+z_i}^{1000} / \partial t$, corresponds to the *net* rate at which POC accumulates in the water column below depths $z_p + z_i$. E_{z_i} can thus be interpreted as the net POC flux at a depth $z_p + z_i$, and E_0 indicates the net POC flux just below the productive layer (i.e., export production). Instantaneous values of E_{z_i} were computed from iPOC values, after application of a pseudo-Gaussian smoothing filter (solid lines in Figure 3). To provide a first-order estimate of seasonal small-particle accumulation in the mesopelagic region, we regressed $iPOC_{z_p}^{1000}$ between the time when $iPOC_0^{1000}$ was minimal (approximately before the maximum in z_m) and the time when $iPOC_{z_p}^{1000}$ reached its seasonal maximum (summer–autumn). A linear least squared model forced through the starting point was used to compute seasonal E_{z_i}. Uncertainties in E_{z_i} were estimated using a Monte Carlo approach (supporting information). Transfer efficiencies of POC flux to a depth z_i below z_p, T_{z_i}, were finally computed as the ratio $E_{z_i} : E_0$ [*Buesseler and Boyd*, 2009].

3. Results

During the 2 years of observations, the floats provided a repeated coverage of the Lofoten Basin (Figure 1). Particle backscattering and the estimated stocks of POC showed consistent seasonal patterns. Both quantities were minimal in January–February, began increasing within the upper productive layer at least a month before the shoaling of the mixed layer in spring, and reached maximum values following this shoaling (Figures 2, 3a, and 3b). In July, the POC stock in the productive layer began decreasing, likely

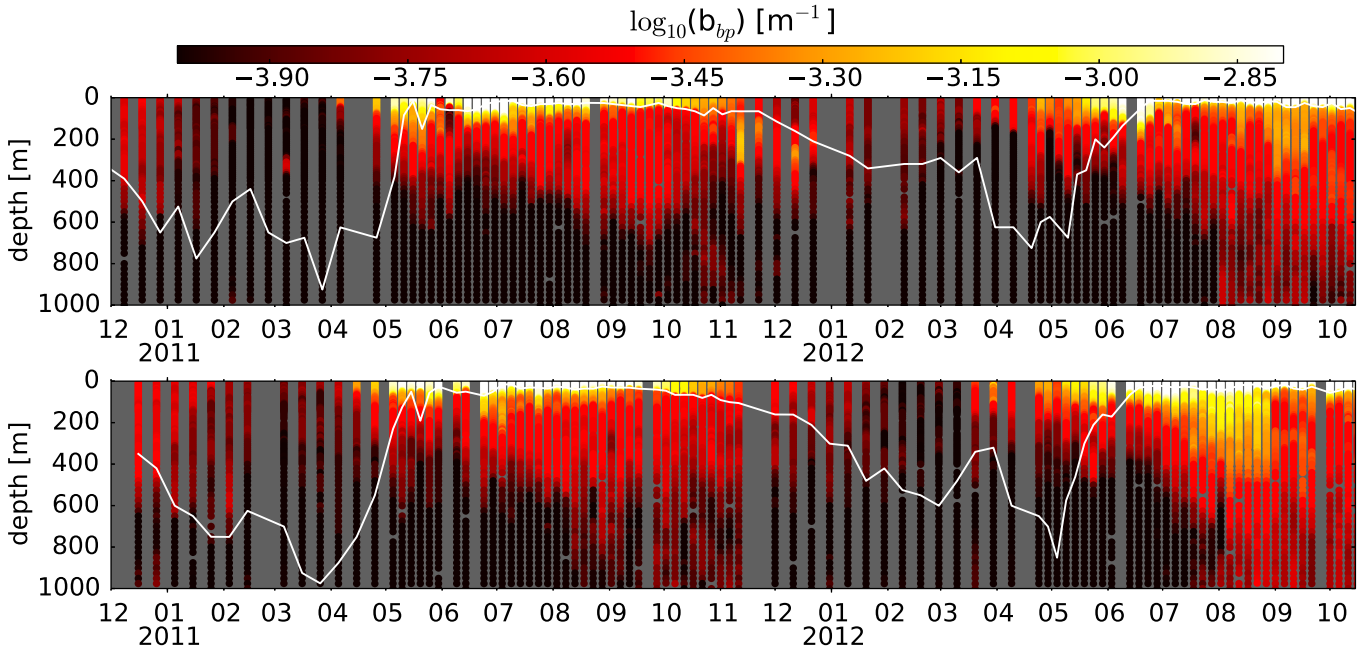

Figure 2. Particulate backscattering, b_{bp}, as a function of depth and time for floats (top) 6900798 and (bottom) 6900799. Note that b_{bp} is plotted on a logarithmic scale. The white continuous line represents an estimate of the mixed layer depth based on a density criterion (i.e., 0.10 kg m^{-3}). Dark gray areas represent missing data.

due to the exhaustion of nutrients [*Bagoien et al.*, 2012], and this decrease continued until the end of the summer.

In the mesopelagic layer, b_{bp} increased at deeper depths as the summer advanced (Figure 2). Integrated POC stocks ($iPOC_{z_i}^{1000}$) began increasing as the mixed layer shoaled in the spring (Figures 3a and 3b). Accumulation of POC then continued throughout the summer until, in the fall, the deepening of the mixed layer marked the beginning of a relatively fast removal of POC from the entire water column. Despite the lower POC concentrations (i.e., b_{bp} values, Figure 2), $iPOC_{z_i}^{1000}$ were comparable to or higher than in the upper

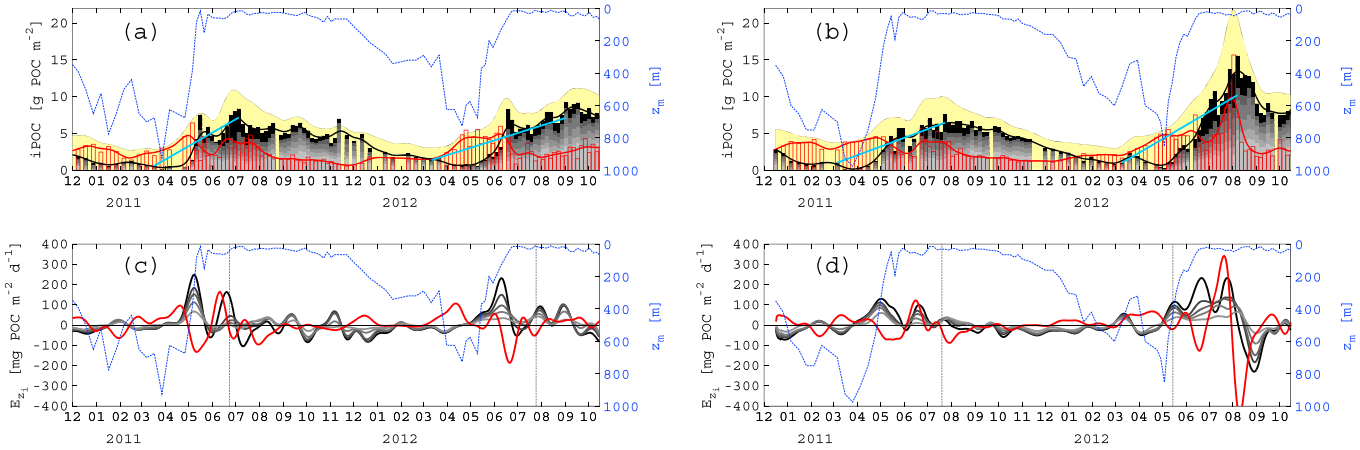

Figure 3. (a and b) Vertically integrated POC stocks (iPOC) in various layers of the water column, for floats 6900798 and 6900799, respectively. Bars: data; solid lines: smoothed data. Red: iPOC in the upper layer. Black: $iPOC_{z_p}^{1000}$. Gray: $iPOC_{z_p+z_i}^{1000}$, with z_i = [50, 100, 200, 300, 400] m and darker grays correspond to smaller z_i. Yellow shaded area: smoothed $iPOC_0^{1000}$. Light blue lines: linear regressions used to estimate seasonal E_0. (c and d) Corresponding instantaneous POC fluxes (E_{z_i}). Red: particle accumulation rates in the productive layer. Black and gray: E_{z_i} just below and at different depths below the productive layer (colors represent depth as for iPOC). Vertical dashed lines: times when the examples instantaneous T_{z_i} presented in Figure 4 were computed. Blue dashed lines are mixed layer depths.

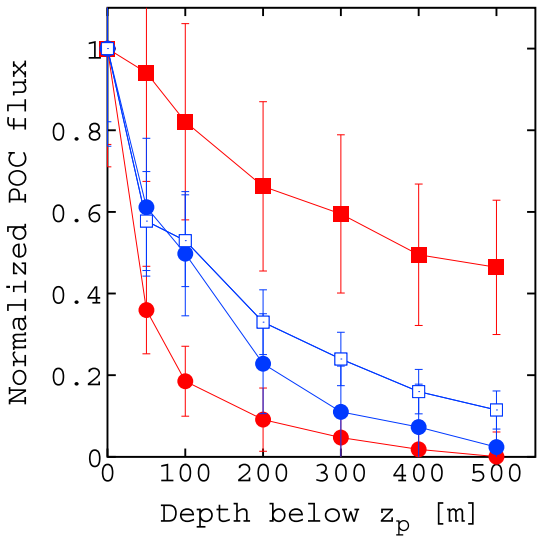

Figure 4. Examples of "instantaneous" estimates of transfer efficiency, i.e., POC flux normalized to the flux at the bottom of the upper productive layer (z_p). Red and blue symbols refer to floats 6900798 and 6900799, respectively. Circles and squares refer to the first and second vertical dashed lines in Figure 3, respectively.

productive layer during summer and fall (Figures 3a and 3b). At the end of the summer, up to 40% of the POC integrated between 0 and 1000 m was found deeper that 400 m below z_p (Figures 3a and 3b).

In July 2012, one of the two floats recorded a large peak in iPOC (Figure 3b) which corresponded to an almost doubling in the surface values of b_{bp}:chl with respect to 2011 (data not shown). Although no other in situ data are available, we hypothesize that this large peak was due to a bloom of coccolithophorids. This hypothesis is supported by MODIS estimates of particulate inorganic carbon (supporting information).

Instantaneous E_{z_i} values showed a large positive peak due to the shoaling of the spring mixed layer, which transferred POC from the productive to the mesopelagic regions (Figures 3c and 3d). One or more positive peaks in E_{z_i} were present during the summer (Figures 3c and 3d). E_{z_i} ranged between 100 and 300 mg C m^{-2} d^{-1} with accumulation rates in the productive region (E_{z_p}) peaking earlier (1–2 weeks, with the exception of the time before the shoaling of z_p) than in the mesopelagic. Note that E_{z_p} is considerably smaller than net primary production, because it includes all particle losses (e.g., grazing and sinking). Instantaneous export production estimates were comparable to values reported in the literature for other ocean regions [e.g., *Buesseler and Boyd*, 2009]. Instantaneous transfer efficiencies 100 m below z_p were variable and ranged between 20% and 80% (see examples in Figure 4).

Seasonal estimates of POC export flux just below (E_0) and 500 m below (E_{500}) the productive layer averaged around 6.7 and 1.5 g C m^{-2} yr^{-1}, respectively (Table 1). Average seasonal estimates of T_{100} and T_{500} were 60% and 23%, respectively (Table 1).

4. Discussion

4.1. Small-Particle Dynamics

Small particles can accumulate in the mesopelagic due to multiple mechanisms. One of the most important is the disaggregation of large sinking particles [*Burd and Jackson*, 2009]. Biological and physical forces can contribute to disaggregation, and both these processes are difficult to observe and to parametrize in models. Our estimates of small-particle fluxes could thus provide important insights regarding the fate of large particles in the mesopelagic. Lateral advection and/or sediment resuspension could also be responsible for the observed b_{bp} signals at depth [*Peinert et al.*, 2001], although the latter is unlikely, because b_{bp} generally

Table 1. Estimates of Seasonal Export Production (g C m^{-2} yr^{-1}) Just Below and 500 m Below the Productive Layer (E_0 and E_{500}, Respectively) and Transfer Efficiencies 100 m and 500 m Below the Productive Layer (T_{100} and T_{500}, Respectively)[a]

	E_0	E_{500}	T_{100}	T_{500}
2011	6.6 ± 0.5	2.2 ± 0.4	0.53 ± 0.07	0.34 ± 0.06
	5.4 ± 0.7	1.1 ± 0.6	0.64 ± 0.11	0.20 ± 0.11
2012	5.8 ± 0.8	1.5 ± 0.2	0.68 ± 0.14	0.27 ± 0.05
	9.1 ± 0.8	1.2 ± 0.3	0.55 ± 0.08	0.13 ± 0.04

[a]In a given year, the first and second rows correspond to floats 6900798 and 6900799, respectively. Errors represent 1 standard deviation.

decreased as a function of depth (Figure 2). Finally, the observed deep b_{bp} values could have been due to small particles sinking from the surface [*Alonso-Gonzalez et al.*, 2010; *Riley et al.*, 2012].

In this study, an additional process appears to have contributed to a significant export of small particles. Figures 3c and 3d show that the largest instantaneous fluxes of small particles were detected in correspondence of the spring shoaling of the mixed layer. Crucially, this shoaling occurred after particles had began accumulating in the upper water column (preshoaling bloom). The particle-laden layer was then isolated from the upper water column by a new shallower mixed layer, resulting in the export of these particles into the mesopelagic region. This physically mediated export process has been previously described and called the "mixed-layer" pump [*Bishop et al.*, 1986; *Ho and Marra*, 1994; *Gardner et al.*, 1995]. In the case of small particles in deeply mixed layers such as those observed in this study, the mixed-layer pump may be responsible for a significant fraction of the annual export. In addition, because particles are mixed relatively deep into the water column, they may escape remineralization. Thus, when mixed layers are deeper than the depth over which most of the remineralization takes place, the mixed-layer pump may be an efficient pathway for carbon export. Finally, because small particles behave similarly to dissolved organic matter (DOM, i.e., they do not sink), we hypothesize that the shoaling of the mixed layer in the spring could be an important mechanism also for exporting the DOM produced before the stratification period.

Independent estimates of export flux from moored sediment traps deployed in the Lofoten Basin are only available for the early 1990s [*Peinert et al.*, 2001]; nevertheless, they provide a useful comparison for our results. In *Peinert et al.* [2001], the particle flux typically peaked between August and October and was in large part (i.e., 50%) composed of calcium carbonate ($CaCO_3$). The mean annual POC flux at 1000 m was 1.9 ± 0.5 g C m^{-2} yr^{-1} [*Peinert et al.*, 2001, Table 3]. Although our data set did not allow us to compute export at 1000 m, maximum particle concentrations inferred from b_{bp} at about 900–1000 m were also found between August and November (Figure 2). Mean seasonal estimates of E_{500} from the floats were 1.6 ± 0.7 and 1.3 ± 0.4 g C m^{-2} yr^{-1} for 2011 and 2012, respectively (Table 1), suggesting that the flux of small particles could represent a considerable component of the POC flux at 500–1000 m. However, because $CaCO_3$ has a higher backscattering per unit of mass than POC [*Gordon et al.*, 2001], our estimates could be overestimated by 44% if, as in *Peinert et al.* [2001], 50% of the flux was due to particles composed of calcite.

Our flux estimates did not include the export of large fast-sinking aggregates [*Briggs et al.*, 2011] and should thus represent only a fraction of the total POC flux at depth. Our method further underestimates export flux, because it does not record a flux under steady state conditions (i.e., when concentrations do not vary, because input fluxes equal removal rates). Finally, our late summer export fluxes could be underestimated, because of a nonnegligible POC flux below 1000 m (see Figure 2). Thus, the estimates presented here should be considered as a lower bound of small-particle fluxes.

It is unclear if the small-particle flux recorded by the backscattering sensors would have been collected by sediment traps. If it was not collected, then our results would indicate that an important component is neglected from current carbon budgets [*Burd et al.*, 2010]. More studies are needed to reconcile the results from these different methodologies.

Calculation of seasonal particle export by this method requires an assumption of spatial homogeneity. Although instantaneous estimates showed variations between the two floats (Figures 3c and 3d), seasonal estimates in the mesopelagic were, in general, consistent within each year (Table 1). However, in the global ocean floats are not confined to specific ocean regions. It is therefore useful to assess the typical spatial scales over which the b_{bp} signals would need to be integrated to achieve accurate carbon flux estimates. By propagating uncertainties in b_{bp} and POC:b_{bp} ratios, we obtained conservative uncertainties in E_{z_i} of about 40%, when we integrated signals over 30 days for a "high-export" scenario (i.e., 100 mg C m^{-2} d^{-1}; supporting information). If a float drifts at depth, in a straight line, and at an average speed of 5.4 cm/s [*Ollitrault and Rannou*, 2013], then during 30 days it would move by about 150 km. Thus, provided that our uncertainty estimates are reasonable, application of the technique presented here to data from a generic float would require an assumption of mesoscale homogeneity. Reducing uncertainties in the POC:b_{bp} ratio would allow us to relax this assumption.

Finally, although our data sets are limited to the upper 1000 m of the water column, the b_{bp} signal propagated at the end of the summer to depths below the deepest winter mixing (Figure 2). Thus, the

particle flux recorded in this study by the backscattering coefficient likely contributed to long-term carbon sequestration.

4.2. Autonomous Platforms and the Ocean Carbon Cycle

An important step toward improving our understanding of the ocean biological carbon pump is to increase the number of carbon flux observations in the upper ocean. The cost and limited spatial coverage of ship-based measurements is a formidable obstacle to such an endeavor. Fortunately, autonomous platforms such as Bio-Argo floats have enormous potential for complementing current observations of carbon flux [e.g., *Bishop and Wood*, 2009].

Bio-optical proxies of particle concentration and characteristics (e.g., POC) carry, by nature, uncertainties due to the underlying empirical conversions. To reduce these uncertainties, more in situ data are needed, especially in the mesopelagic region. Nonetheless, few, if any, other measurements can parallel the spatiotemporal coverage that optical proxies afford when recorded by autonomous platforms in situ (or from space). These data can complement existing measurements and help resolve current method-method uncertainties in estimating carbon export.

Data from Bio-Argo floats have already demonstrated that multiyear, high-resolution, vertically resolved observations can transform the way we understand ocean ecosystems and biogeochemistry [*Bishop et al.*, 2004; *Riser and Johnson*, 2008; *Boss and Behrenfeld*, 2010; *Johnson et al.*, 2010; *Estapa et al.*, 2013]. The results presented here provide another example of how a global fleet of Bio-Argo floats could allow us a quantum leap in understanding of the ocean carbon cycle.

5. Conclusions

(1) Optical backscattering data from Bio-Argo floats unveiled the seasonal dynamics of small particles in the upper 1000 m of the Norwegian Sea.
(2) In the summer and autumn the integrated POC stocks of small particles in the mesopelagic were comparable to or greater than in the upper productive layer.
(3) The shoaling of the mixed layer in the spring was important for exporting small-particle carbon.
(4) Estimates of small-particle POC export were comparable to literature values determined by sediment traps.
(5) Small particles contributed to long-term carbon sequestration.

Acknowledgments

S. Saux-Picard and T. Kristiansen are acknowledged for their help in preparing Figure 1. E. Boss and N. Briggs are thanked for discussions on spikes in optical measurements. L. Polimene, D. Raitsos, J. Bishop, and, especially, an anonymous reviewer are thanked for their comments on an earlier version of this paper. These data were collected and made freely available by the International Argo Program and the national programs that contribute to it (http://www.argo.ucsd.edu, http://argo.jcommops.org). The Argo Program is part of the Global Ocean Observing System. G.D.O. acknowledges funding from the UK National Centre for Earth Observation and Marie Curie FP7-PIRG08-GA-2010-276812.

The Editor thanks James Bishop and an anonymous reviewer for their assistance in evaluating this paper.

References

Alonso-Gonzalez, I. J., J. Aristegui, C. Lee, A. Sanchez-Vidal, A. Calafat, J. Fabres, P. Sangra, P. Masque, A. Hernandez-Guerra, and V. Benitez-Barrios (2010), Role of slowly settling particles in the ocean carbon cycle, *Geophys. Res. Lett.*, *37*, L13608, doi:10.1029/2010GL043827.

Bagoien, E., W. Melle, and S. Kaartvedt (2012), Seasonal development of mixed layer depths, nutrients, chlorophyll and Calanus finmarchicus in the Norwegian Sea—A basin-scale habitat comparison, *Prog. Oceanogr.*, *103*, 58–79, doi:10.1016/j.pocean.2012.04.014.

Bishop, J. K. B., M. H. Conte, P. H. Wiebe, M. R. Roman, and C. Langdon (1986), Particulate matter production and consumption in deep mixed layers: Observations in a warm-core ring, *Deep Sea Res. Part A*, *33*, 1813–1841.

Bishop, J. K. B., T. J. Wood, R. E. Davis, and J. T. Sherman (2004), Robotic observations of enhanced carbon biomass and export at 55 degrees S during SOFeX, *Science*, *304*(5669), 417–420.

Bishop, J. K. B., and T. J. Wood (2009), Year-round observations of carbon biomass and flux variability in the Southern Ocean, *Global Biogeochem. Cycles*, *23*, GB2019, doi:10.1029/2008GB003206.

Boss, E., and M. Behrenfeld (2010), In situ evaluation of the initiation of the North Atlantic phytoplankton bloom, *Geophys. Res. Lett.*, *37*, L18603, doi:10.1029/2010GL044174.

Briggs, N., M. J. Perry, I. Cetinic, C. Lee, E. D'Asaro, A. M. Gray, and E. Rehm (2011), High-resolution observations of aggregate flux during a sub-polar North Atlantic spring bloom, *Deep Sea Res. Part I*, *58*(10), 1031–1039.

Buesseler, K. O., and P. W. Boyd (2009), Shedding light on processes that control particle export and flux attenuation in the twilight zone of the open oceans, *Limnol. Oceanogr.*, *54*(4), 1210–1232, doi:10.4319/lo.2009.54.4.1210.

Burd, A. B., and G. A. Jackson (2009), Particle aggregation, *Annu. Rev. Mar. Sci.*, *1*, 65–90, doi:10.1146/annurev.marine.010908.163904.

Burd, A. B., et al. (2010), Assessing the apparent imbalance between geochemical and biochemical indicators of meso- and bathypelagic biological activity: What the @$#! is wrong with present calculations of carbon budgets?, *Deep Sea Res. Part II*, *57*, 1557–1571.

Cetinić, I., M. J. Perry, N. T. Briggs, E. Kallin, E. A. D'Asaro, and C. M. Lee (2012), Particulate organic carbon and inherent optical properties during 2008 North Atlantic Bloom Experiment, *J. Geophys. Res.*, *117*, C06028, doi:10.1029/2011JC007771.

Dall'Olmo, G., E. Boss, M. Behrenfeld, and T. Westberry (2012), Particulate optical scattering coefficients along an Atlantic meridional transect, *Opt. Express*, *20*(19), 21,532–21,551.

Estapa, M. L., K. Buesseler, E. Boss, and G. Gerbi (2013), Autonomous, high-resolution observations of particle flux in the oligotrophic ocean, *Biogeosciences*, *10*(8), 5517–5531.

Gardner, W. D., S. P. Chung, M. J. Richardson, and I. D. Walsh (1995), The oceanic mixed-layer pump, *Deep Sea Res.*, *42*(2–3), 1587–1590.

Gordon, H. R., G. C. Boynton, W. M. Balch, S. B. Groom, D. S. Harbour, and T. J. Smyth (2001), Retrieval of coccolithophore calcite concentration from SeaWiFS imagery, *Geophys. Res. Lett.*, *28*(8), 1587–1590.

Henson, S. A., R. Sanders, E. Madsen, P. J. Morris, F. Le Moigne, and G. D. Quartly (2011), A reduced estimate of the strength of the ocean's biological carbon pump, *Geophys. Res. Lett.*, *38*, L04606, doi:10.1029/2011GL046735.

Ho, C., and J. Marra (1994), Early-spring export of phytoplankton production in the northeast Atlantic Ocean, *Mar. Ecol. Prog. Ser.*, *114*, 197–202.

Johnson, K. S., S. C. Riser, and D. M. Karl (2010), Nitrate supply from deep to near-surface waters of the North Pacific subtropical gyre, *Nature*, *465*(7301), 1062–1065, doi:10.1038/nature09170.

Laws, E. A., P. G. Falkowski, W. O. Smith, H. Ducklow, and J. J. McCarthy (2000), Temperature effects on export production in the open ocean, *Global Biogeochem. Cycles*, *14*(4), 1231–1246.

Ollitrault, M., and J. P. Rannou (2013), ANDRO: An Argo-based deep displacement dataset, *J. Atmos. Oceanic Technol.*, *30*, 759–788.

Peinert, R., A. Antia, E. Bauerfeind, B. von Bodungen, O. Haupt, M. Krumbholz, I. Peeken, R. Ramseier, M. Voss, and B. Zietzschel (2001), Particle flux variability in the polar and Atlantic biogeochemical provinces of the Nordic Seas, in *The Northern North Atlantic*, edited by P. Schäfer et al., pp. 53–68, Springer, Berlin, Heidelberg.

Riley, J. S., R. Sanders, C. Marsay, F. A. C. Le Moigne, E. P. Achterberg, and A. J. Poulton (2012), The relative contribution of fast and slow sinking particles to ocean carbon export, *Global Biogeochem. Cycles*, *26*, GB1026, doi:10.1029/2011GB004085.

Riser, S. C., and K. S. Johnson (2008), Net production of oxygen in the subtropical ocean, *Nature*, *451*(7176), 323–325, doi:10.1038/nature06441.

Stramski, D., E. Boss, D. Bogucki, and K. J. Voss (2004), The role of seawater constituents in light backscattering in the ocean, *Prog. Oceanogr.*, *61*(1), 27–56.

Trull, T., S. Bray, K. Buesseler, C. Lamborg, S. Manganini, C. Moy, and J. Valdes (2008), In situ measurement of mesopelagic particle sinking rates and the control of carbon transfer to the ocean interior during the vertical flux in the global ocean (Vertigo) voyages in the North Pacific, *Deep Sea Res. Part II*, *55*(14-15), 1684–1695.

Voet, G., D. Quadfasel, K. A. Mork, and H. Soiland (2010), The mid-depth circulation of the Nordic Seas derived from profiling float observations, *Tellus Ser. A*, *62*(4), 516–529, doi:10.1111/j.1600-0870.2010.00444.x.